Eur Biophys J 21, 63–70 (1992)

European Biophysics Journal

Conformational transition of an α-helix studied by molecular dynamics

J. Pleiss* and F. Jähnig

Max-Planck-Institut für Biologie, Correnstrasse 38, W-7400 Tübingen, Federal Republic of Germany

Received July 29, 1991/Accepted in revised form December 12, 1991

Abstract. Molecular dynamics simulations were performed on a 20-residue polyalanine helix and a spontaneous transition from a kinked to a straight conformation was observed. The kinetics of the transition was analyzed within the framework of the Kramers model for chemical reactions and within a random walk model. The Kramers model which is based on diffusion along a one-dimensional reaction pathway and the crossing of an energy barrier was found to be inadequate. Instead, a random walk model based on diffusion in the high-dimensional phase space of the system was found to be compatible with the data. The high dimensionality of the phase space permits the system to circumvent high energy barriers and diffuse rapidly at about constant energy, but decelerates the reaction since in the labyrinth of pathways the transition state is reached rarely.

Key words: Protein folding – Protein dynamics – Kramers theory – Random walk – Diffusion

Introduction

Folding of a protein into its native structure involves a series of structural transitions. Which transitions occur in which order is not known and different models have been suggested (Karplus and Weaver 1976; Jaenicke 1987). In one model, the diffusion-collision model, the secondary structure elements of the native structure are formed first, then these microdomains undergo diffusion and collisions until the appropriate microdomains coalesce and the ensemble of microdomains folds into the native tertiary structure. Obviously, in this model the intervening segments between the secondary structure elements provide the necessary flexibility for folding, they undergo conformational transitions. Recently, experimental evidence for the early formation of secondary structure elements has been presented (Udgaonkar and Baldwin 1988; Roder et al. 1988).

Structural transitions are also required for the proper functioning of proteins as catalysts (Frauenfelder et al. 1988). A hierarchical model has been postulated for such transitions (Ansari et al. 1989). In this model, the lowest order transitions involve the crossing of low energy barriers and thus occur frequently. They lead to higher order transitions across higher energy barriers which occur less frequently. This continues until, finally, the structural transition involved in catalysis occurs. Again the intervening segments between secondary structure elements are supposed to serve as the flexible links in the structural transitions (Elber and Karplus 1987). Experimental evidence for such a hierarchical model has been presented (Dornmair and Jähnig 1989).

Hence, conformational transitions in the segments connecting the secondary structure elements seem to play a central role in the folding and functioning of proteins. For a better understanding of these processes, therefore, knowledge of the exact pathways of such transitions and of the rate-limiting steps involved would be useful. The folding dynamics of two α-helices connected by a random-coil polypeptide chain have been studied (Lee et al. 1987). The helices underwent diffusion, and folding was defined as the coalescence of the two. The intervening segment was found to have a pronounced effect on the diffusion of the helices. It slowed down the diffusion and thus the rate of folding. However, the exact diffusion pathway and the energy profile along the path specifying the rate-limiting steps were not investigated.

To a first approximation, conformational transitions in proteins may be considered as chemical reactions and their kinetics be described by chemical reaction models (Kramers 1940; Northrup and Hynes 1980; Schulten et al. 1981; Lee and Karplus 1988), preferentially the Kramers model (Kramers 1940). This model is based on the diffusive crossing of an energy barrier and requires the following assumptions to be fulfilled: (*i*) The system is in thermal equilibrium during the entire transition, (*ii*) a

---

* *Present address:* Biostructure S.A., Les Algorithmes-Parc d'Innovation, F-67400 Illkirch-Graffenstaden, France

Offprint requests to: F. Jähnig

unique one-dimensional reaction path can be defined, and (*iii*) the energy profile along the reaction path has a dominant energy barrier higher than thermal energy. For conformational transitions in proteins, the first condition may be fulfilled, since the atomic fluctuations are fast and restore thermal equilibrium in times much shorter than the time required for a conformational transition. Whether or not the second condition can be fulfilled is an open question, since conformational transitions in proteins in general involve changes of a large number of degrees of freedom so that the definition of a one-dimensional reaction coordinate is not obvious. If the number of degrees of freedom is high, the third condition can also hardly be fulfilled. A high energy barrier which exists along one degree of freedom can always be circumvented by altering another degree of freedom. In summary, there is no guarantee for the applicability of the Kramers model to conformational transitions in proteins.

In special cases, a reaction coordinate may be defined, an example being the 180° flip of a tyrosine side chain in bovine pancreatic trypsin inhibitor (Gelin and Karplus 1975; Ghosh and McCammon 1987). Here, the rotation angle of the side chain may serve as reaction coordinate. The energy profile as a function of this angle was calculated and an energy barrier was found in rough agreement with the experimental result. In the general case, however, the definition of a reaction coordinate is more difficult. One strategy, therefore, is to investigate the energy landscape of a protein in the high-dimensional phase space of all degrees of freedom and to find the pathway with the lowest energy barrier between the initial and final structure (Czerminski and Elber 1989). For computational reasons, this is possible only for small polypeptides. For a tetrapeptide, about 1000 alternative pathways differing by energies of not more than thermal energy were found. Hence, a unique pathway is difficult to define even for a small polypeptide. Another strategy to find the possible pathways and to define a reaction coordinate is to perform molecular dynamics (MD) simulations. In general, this is again not feasable for proteins, since MD simulations can only be extended over times of the order of ns, while most structural transitions in proteins require much longer times. So again one is restricted to small polypeptides or parts of proteins. An advantage of MD simulations lies in the possibility to accelerate the sampling of phase space by raising the temperature. A conformational transition involving a loop of triosephosphate isomerase could be studied in this way by keeping the rest of the protein fixed and increasing the temperature to 1000 K (Joseph et al. 1990). One of the findings was the absence of a large energy barrier between the initial and final states of the transition.

In our work we followed a similar strategy. We used a relatively small system, a 20-residue polyalanine helix, and studied the transition between a kinked and the straight conformation by MD simulations. To increase the sampling efficiency, we applied a strong coupling of the helix to a heat bath at 300 K (Berendsen et al. 1984). Our aim was to find out what determines the rate of this conformational transition. For this purpose, we tried to answer the following questions: (*i*) Is it possible to assign a reaction coordinate and a unique pathway to the transition? (*ii*) Are there high energy and/or entropy barriers along the reaction pathway which have to be overcome during the transition? (*iii*) If there are no barriers, what effect prevents the transition from occurring instantaneously?

Methods

MD simulation technique

Energy minimization and MD simulations were performed using the program GROMOS (W. F. van Gunsteren and H. J. C. Berendsen, BIOMOS B. V., University of Groningen, Groningen, Netherlands). In all MD simulations the bond lengths are constrained by the SHAKE algorithm (Ryckaert et al. 1977). Then the standard GROMOS force field is a sum of terms involving bond angles, dihedrals, improper dihedrals, and terms describing the non-bonded electrostatic and Lennard-Jones interactions (van Gunsteren and Karplus 1982). This force field is extended by an additional 10–12 potential to explicitely include hydrogen bond interactions (van Gunsteren and Karplus 1982). The electrostatic interaction is calculated by taking into account only neutral charge groups and a dielectric constant of 1. For all non-bonded interactions a cutoff of 1 nm is used with the neighbour list updated every 10 time steps. The time step is chosen as 2 fs. Coordinates are stored at every 20 time steps. To couple the helix to an external heat bath the algorithm of Berendsen et al. (1984) was adopted. After each integration step, the temperature of the helix is calculated from the velocities of the atoms. If it deviates from 300 K, the velocities are rescaled with a relaxation time τ_C. Two values for τ_C are used: $\tau_C = 100$ fs for weak coupling, and $\tau_C = 10$ fs for strong coupling. The MD simulations are perfomed on a μVAX II and a CRAY-XMP.

Full MD simulation

Regular α-helices of $(\text{Ala})_{20}$ and $(\text{Ala})_{10}$-Pro-$(\text{Ala})_9$ are generated. Kinked conformations are obtained by changing the three backbone dihedrals (Φ_{10}, Ψ_{10}, Φ_{11}) from the regular angles (−57°, −47°, −57°) to (−147°, 80°, −20°). The kink angle is determined as described previously (Pleiss and Jähnig 1991).

The kinked conformations are energy-minimized by a steepest-descent algorithm and heated to 300 K by a 2 ps MD simulation under strong coupling to a heat bath. The resulting coordinates of the peptide atoms provide the initial conformation for further MD simulations. The initial velocities of the atoms for these simulations are either taken unchanged from the heating runs or are assigned new values generated randomly with the restriction to obey a Maxwell distribution. The MD simulations are performed under weak or strong coupling to a heat bath at 300 K are extended over times ranging up to 700 ps.

Reaction coordinate model

A typical kinked conformation of $(\mathrm{Ala})_{20}$ is picked from an MD trajectory. The values of $(\Phi_{10}, \Psi_{10}, \Phi_{11})$ in this conformation are determined as $(\Phi^i_{10}, \Psi^i_{10}, \Phi^i_{11}) = (-83°, 83°, -38°)$, the other backbone dihedrals being near their α-helical values. In the straight conformation, the values of the three dihedrals are $(\Phi^f_{10}, \Psi^f_{10}, \Phi^f_{11}) = (-57°, -47°, -57°)$. Different reaction paths between the initial and final conformations are investigated. In a first approach, the three dihedrals $(\Phi_{10}, \Psi_{10}, \Phi_{11})$ are assumed to vary linearly along the reaction path according to

$$\Phi_{10} = \Phi^i_{10} + (\Phi^f_{10} - \Phi^i_{10})\,\xi$$
$$\Psi_{10} = \Psi^i_{10} + (\Psi^f_{10} - \Psi^i_{10})\,\xi$$
$$\Phi_{11} = \Phi^i_{11} + (\Phi^f_{11} - \Phi^i_{11})\,\xi,$$

thereby defining a reaction coordinate ξ with $0<\xi<1$. The reaction path is split up into 20 steps so that ξ increases in steps of 0.05 along the path. At each step, the values of $(\Phi_{10}, \Psi_{10}, \Phi_{11})$ are fixed and the other coordinates relaxed by a steepest-descent energy minimization and a 12 ps MD simulation under weak coupling to a heat bath at 10 K. Fixation of $(\Phi_{10}, \Psi_{10}, \Phi_{11})$ at their respective values is achieved by imposing a harmonic potential of strength $K = 1000$ kJ/mol · grad^2 (Northrup et al. 1982). The potential energy is averaged between 4 and 12 ps to provide the mean potential energy as a function of ξ.

In a second approach, the reaction path is taken from the MD simulation. The trajectory contains the helix conformations at every 40 fs. Fifty conformations covering 2 ps in the region of the conformational transition are individually subjected to 8 ps MD simulations under weak coupling to a heat bath at 10 K with the dihedrals $(\Phi_{10}, \Psi_{10}, \Phi_{11})$ fixed at their values given by the trajectory. In this way, the other degrees of freedom are relaxed. Averaging between 4 ps and 8 ps yields the mean potential energy along the reaction path.

The third approach is similar to the second one except that in the 8 ps MD simulations at 10 K, instead of the three dihedrals $(\Phi_{10}, \Psi_{10}, \Phi_{11})$, the 13 dihedrals $(\Phi_7, \Psi_7, \ldots, \Phi_{13})$, are fixed at their values given by the trajectory.

Results and discussion

Conformational transition

We started from a regular α-helix of $(\mathrm{Ala})_{20}$ and changed the three backbone dihedrals $(\Phi_{10}, \Psi_{10}, \Phi_{11})$ from their α-helical values (−57°, −47°, −57°) to (−147°, 80°, −20°), thereby introducing a right-angled kink in the middle of the helix. The kinked helix was energy-minimized and then heated up to 300 K. In the resulting conformation, the three dihedrals had changed to average values of (−95°, 82°, −25°) and the kink angle to 107°. This kinked conformation was used as initial structure for an MD simulation. The time courses of the kink angle and of the three dihedrals $(\Phi_{10}, \Psi_{10}, \Phi_{11})$ are shown in Figs. 1 A and B. For more than 100 ps, the kink angle oscillates about the mean value of 107° with a period of about 5 ps. These oscillations are typical for the bending vibration of such a helix (Pleiss and Jähnig 1991) and indicate that the system is in a local energy minimum. At about 115 ps, the dihedrals spontaneously change to their α-helical values and the kink angle to nearly 0°, i.e. the helix undergoes a transition from the kinked to the straight conformation. From Fig. 1 A one might get the impression that the occurrence of the transition is correlated with an increase of the bending vibration in amplitude, but such a correlation has not been observed in other simulations. It should also be noted that in the kinked conformation each of the three dihedrals exhibits strong fluctuations, but in general they do not fit together to permit the transition. After the transition, the helix again exhibits bending vibrations and fluctuations of the three dihedrals, although with a smaller amplitude than before. This is indicative of a deeper energy minimum.

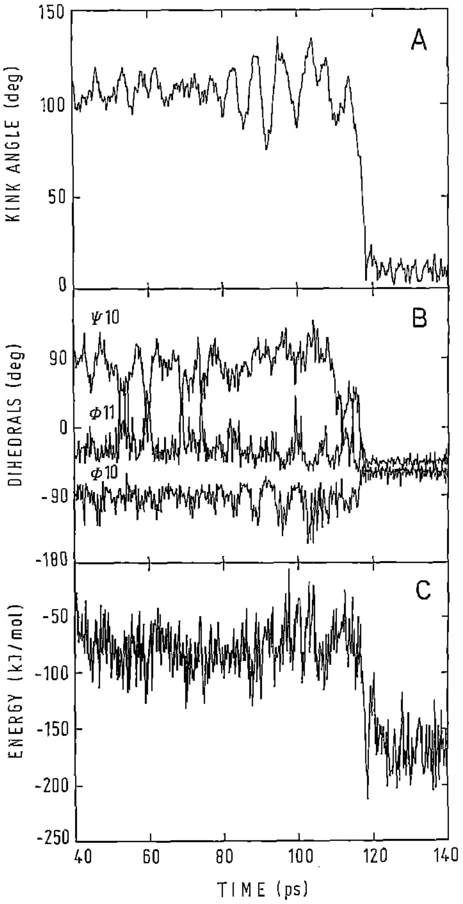

Fig. 1. Time dependence of the kink angle (A), of the three dihedrals $(\Phi_{10}, \Psi_{10}, \Phi_{11})$ (B), and of the total potential energy (C) of the $(\mathrm{Ala})_{20}$-helix under strong coupling to a heat bath at 300 K

The time course of the potential energy is shown in Fig. 1 C. At the beginning the energy fluctuates about a mean value of approximately −80 kJ/mol, and after the conformational transition about a value of approximately −160 kJ/mol, i.e. the energy of the straight conformation is lower than that of the kinked conformation by about 80 kJ/mol. There is no obvious energy barrier to be overcome during the transition, but it might be hidden in the fluctuations.

To get a mean value for the transition rate k^{tr} or the reaction time $\tau^{tr} = 1/k^{tr}$, the simulation was repeated several times starting from the same initial structure, but different initial velocities of the atoms. In 2 out of 9 simulations, no transition occurred within 450 ps, but the helix partially unfolded at both ends in 1 simulation the kinked helix adopted a hairpin conformation after 430 ps, and in the remaining 6 simulations a transition to the straight helix took place after times ranging from 75 ps to 250 ps. Obviously, for the kinked helix three different pathways exist: (*i*) It may partially unfold, (*ii*) adopt a hairpin conformation, or (*iii*) adopt a straight conformation which is the most stable one. We will be concerned only with the third pathway. Its mean reaction time resulted as $\tau^{tr} = 150 \pm 100$ ps.

To test the general validity of these results, a slightly different system was studied, namely the 20-residue helix $(\mathrm{Ala})_{10}$-Pro-$(\mathrm{Ala})_9$. For this helix, a kinked conformation has previously been predicted as the most stable structure (Piela et al. 1987). The same procedure as above for the $(\mathrm{Ala})_{20}$-helix was applied to the $(\mathrm{Ala})_{10}$-Pro-$(\mathrm{Ala})_9$-helix. Nine MD simulations were performed and in all cases the helix underwent a transition to a hairpin conformation with a kink angle of nearly 180°. The mean potential energy of this conformation was slightly lower than that of the kinked conformation and again there was no obvious energy barrier between the initial and the final conformation. The reaction time resulted as $\tau^{tr} = 60 \pm 40$ ps.

Since the conformational transition of the $(\mathrm{Ala})_{10}$-Pro-$(\mathrm{Ala})_9$-helix occurred relatively fast, it could be used for another test. In the simulations presented up to now, the helices had been coupled strongly to a heat bath at 300 K. We now reduced the strength of this coupling by increasing the relaxation time of the coupling from 10 fs to 100 fs. Under such weak coupling, the transition from the kinked to the hairpin conformation of the $(\mathrm{Ala})_{10}$-Pro-$(\mathrm{Ala})_9$-helix occurred after 470 ps, which is nearly an order of magnitude longer than for strong coupling. When a simulation of the kinked $(\mathrm{Ala})_{20}$-helix was performed under weak coupling, no transition was found within 700 ps. By analogy to the case of the $(\mathrm{Ala})_{10}$-Pro-$(\mathrm{Ala})_9$-helix, one would expect the reaction time for the kinked-straight transition of the $(\mathrm{Ala})_{20}$-helix to be about 10 times longer for weak coupling than for strong coupling, i.e. about 1.5 ns.

Two remarks should be added. (*i*) Our simulations are vacuum simulations which implies that in lack of surrounding water molecules the system tries to maximize the number of intramolecular van der Waals interactions and to adopt a more globular shape, such as for example the hairpin conformation. The tendency to adopt this conformation may thus be an artefact of the vacuum character of the simulations. (*ii*) Surrounding water molecules also affect the dynamic behavior of the helices. Collisions with the helix atoms may act accelerating on the helix atoms giving rise to thermal motion and may act decelerating giving rise to damping. These dynamic effects can be simulated in rough approximation by coupling the helices to a heat bath (Berendsen et al. 1984). Obviously, such a coupling does not affect the energy surface of the helices, it may however alter the population density on this surface and thus the entropy. As shown previously, the latter effect is small for weak coupling of the helices to the heat bath, i.e. for a relaxation time of 100 fs (Berendsen et al. 1984). However, strong coupling with a relaxation time of 10 fs as often used by us, may give rise to artefacts in the entropy.

Reaction coordinate model

In attempting to define a reaction coordinate for the transition from the kinked to the straight helix, an obvious choice would be the kink angle. Since, however, on an atomic level the kink angle is a function of the backbone dihedrals and in our case was adjusted by altering the three angles (Φ_{10}, Ψ_{10}, Φ_{11}), we chose a reaction coordinate ξ related linearly to changes of these three angles. As shown in Fig. 2A, when ξ varies from 0 to 1 along the reaction path, the three dihedrals vary from their values in the kinked conformation to those in the straight conformation. It is obvious that due to the coupling between the three dihedrals and the kink angle, ξ is also a rough measure for the kink angle. The reaction path between $\xi = 0$ and $\xi = 1$ was split up into 20 steps. Starting from the initial conformation, after each step a short MD run at 10 K was performed with the three dihedrals kept fixed. This procedure essentially represents an energy minimization with respect to the other degrees of freedom. Permitting them to relax to the ground state, the fluctuating part of their potential energy is eliminated and the potential energy as a function of the reaction coordinate is obtained. The result is shown in Fig. 2B. The energies of the initial and final states differ by about 80 kJ/mol, as known already from the full MD simulation. In the MD simulation, an energy barrier between the two states was

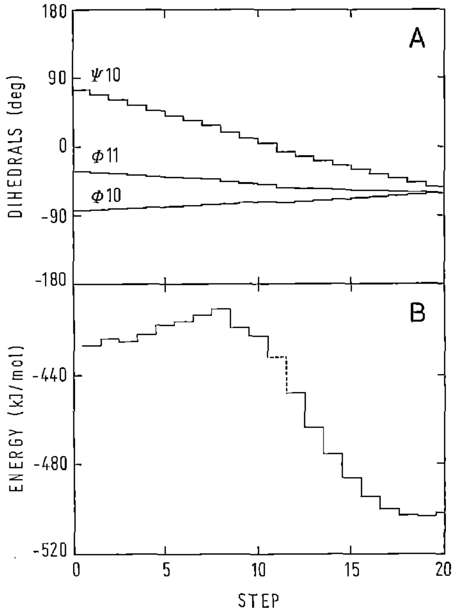

Fig. 2. Variation of the three dihedrals (Φ_{10}, Ψ_{10}, Φ_{11}) (**A**) and of the corresponding total potential energy (**B**) along an arbitrary stepwise transition from the kinked (step 0) to the straight (step 20) conformation of the $(\mathrm{Ala})_{20}$-helix. In one case indicated by dashed lines in (**B**) the simulation did not stabilize at the nearby local minimum as in the other cases but led to a structure with a much lower energy

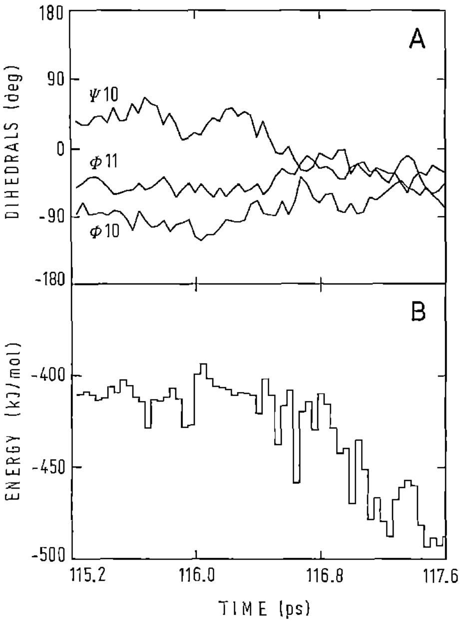

Fig. 3. Variation of the three dihedrals (Φ_{10}, Ψ_{10}, Φ_{11}) (**A**) across the kinked-straight transition of the $(\text{Ala})_{20}$-helix as obtained from the MD simulation. The total potential energy (**B**) was obtained by keeping these three dihedrals fixed and relaxing the other degrees of freedom

not recognizable, while now the two states are clearly separated by an energy barrier of about 20 kJ/mol.

To test this result, the full MD simulation was used to determine the exact energy profile along the reaction path. Still the reaction path was assumed to be specified by the three dihedrals (Φ_{10}, Ψ_{10}, Φ_{11}), but it was no longer given by varying these angles linearly between their initial and final values (Fig. 2 A). Instead, the values of the three dihedrals across the transition region were taken from the MD simulation (Fig. 3 A). In principle, a reaction coordinate ξ could still be defined, but the three dihedrals would be extremely complicated functions of it. To determine the energy profile along this path as good as possible, the other degrees of freedom were no longer taken just from the initial conformation, but were also varied along the reaction path as given by the MD simulation. The MD trajectory contains the helix conformations at every 40 fs. Each of these conformations was subjected to a short MD run at 10 K with the three dihedrals (Φ_{10}, Ψ_{10}, Φ_{11}) kept fixed. As mentioned above, this procedure permits the other degrees of freedom to relax to the ground state and yields the energy profile along the reaction path. The result is shown in Fig. 3 B. The energy difference between the initial and final states is again about 80 kJ/mol, but there is no longer a pronounced energy barrier as in Fig. 2 B. This finding is a major result of the present work. Besides, it should be noted that the energy in Fig. 3 B fluctuates more strongly than in Fig. 2 B. Especially striking is the large number of energy minima with depths reaching 30 kJ/mol. This energy is much higher than the thermal energy of the three dihedrals which is 7.5 kJ/mol, hence an escape from the minima would be nearly impossible. This suggests that too many coordinates were permitted to relax thereby lowering the energy in the minima too much and keeping the available thermal energy of the unrelaxed degrees of freedom too small.

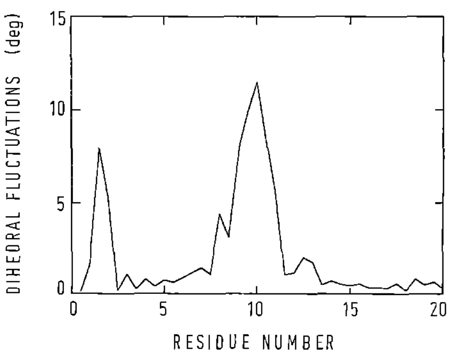

Fig. 4. Fluctuations of the 20 dihedrals (Φ_i, Ψ_i) during the kinked-straight transition of the $(\text{Ala})_{20}$-helix. The difference between the values of each dihedral at consecutive time steps was determined and averaged across the transition region

To study this problem in more detail, we determined the variation of all backbone dihedrals of the $(\text{Ala})_{20}$-helix along the MD trajectory in the transition region. The result is shown in Fig. 4. Apart from irrelevant changes at the *N*-terminal end, 13 dihedrals in the middle of the helix undergo changes. Hence, not only the three dihedrals (Φ_{10}, Ψ_{10}, Φ_{11}) change during the transition, but 10 more dihedrals participate although with smaller amplitudes. The participation of more dihedrals in the transition is conceivable since the dihedrals along the helix backbone are strongly coupled (Pleiss and Jähnig 1991). In a final approach, therefore, we chose a reaction path specified by the 13 backbone dihedrals ($\Phi_7, \ldots, \Phi_{13}$). The conformations of the MD trajectory were subjected to short MD runs at 10 K with the 13 dihedrals kept fixed. In this way, the other degrees of freedom were again relaxed. The fact that their values were also taken from the MD trajectory is irrelevant since they do not contribute to the transition and one might as well have attributed to them their values in the initial conformation. The energy minima are essentially of the same kind as before (Fig. 3 B). Since, however, the thermal energy of the 13 dihedrals is larger, namely 32.5 kJ/mol, the minima can now be left again when the system proceeds along the reaction path. Hence, high energy barriers are not determining the reaction time.

In the absence of a high energy barrier, the reaction time might be governed by an entropy barrier (corresponding to a region of low entropy), which has to be surmounted when the system proceeds along the reaction pathway. Assuming fast relaxation to local equilibrium of all degrees of freedom, the entropy along the pathway can be estimated. Such an assumption is compatible with the Kramers model which is based on the existence of local equilibrium along the entire reaction path. To estimate the entropy at each time step we adopted the method of Karplus and Kushick (1981). They calculated the entropy of an equilibrium state by assuming a Gaussian distribution for each internal variable and determined the width of the distribution, the thermal fluctuations, by averaging in time. To calculate the entropy of the system at each time step the temporal average has to be replaced by an ensemble average. We therefore determined the width of

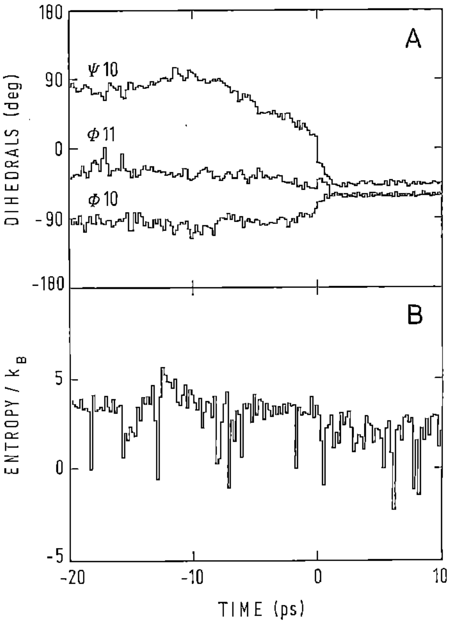

Fig. 5. Variation of the dihedrals ($\Phi_{10}, \Psi_{10}, \Phi_{11}$) (**A**) across the kinked-straight transition obtained as an average over the 6 MD simulations after shifting the transitions to time $t_0 = 0$. The variation of the relative entropy in units of the Boltzmann constant k_B is shown in (**B**)

the Gaussian distribution for each internal variable by averaging over the six MD runs. Before doing so, the conformational transitions observed in the different runs were shifted in time so that they all occurred at the same time t_0. The mean values of the three dihedrals (Φ_{10}, Ψ_{10}, Φ_{11}) are shown in Fig. 5 A, and the entropy calculated from the fluctuations of all internal variables is shown in Fig. 5 B. The mean dihedrals vary in time qualitatively similar to the dihedrals for one run (Fig. 1 B), but as expected exhibit smaller fluctuations. The entropy fluctuates rather strongly as a consequence of the small ensemble of only 6 runs used to calculate it. Despite of these strong fluctuations, it is evident that (*i*) the entropy is higher for the kinked helix than for the straight helix, and (*ii*) an entropy well at the transition is absent. The difference in entropies at the transition yields $T\Delta S = 5$ kJ/mol, much smaller than the difference in energy. This behavior has been noted previously by others (Lee and Karplus 1988). Although the result for the entropy is only a rough estimate, owing to the strong coupling of the helix to a heat bath and the assumption of local equilibrium along the reaction pathway, the absence of any pronounced entropy well implies that the reaction time is governed neither by an energy barrier nor by an entropy barrier.

Random walk model

What determines the reaction time of the conformational transition in the absence of high energy or entropy barriers? Without doubt such barriers exist, but the system seems to circumvent them. This is possible because of the high dimensionality of the energy landscape of the system. If, while diffusing along one variable in phase space the system meets a high energy barrier, it may stop altering this variable and instead alter another variable, i.e. diffuse in another direction and thus avoid crossing the high barrier. Thus, the system performs a random walk on the energy landscape by following the valleys at about constant energy. Only small energy barriers of height up to thermal energy are overcome. Hence, the random walk is nothing else than the superposition of the thermal fluctuations of all internal variables. The difficulty for a conformational transition to occur lies in the requirement that many variables simultaneously undergo a fluctuation in a distinct direction leading to a distinct transition state. Once the transition state is reached, the system does not return to the old conformation but approaches a new conformation with a lower energy.

To get an estimate for the transition rate within the framework of this model, one may assume, as discussed above in connection with the entropy, that each internal variable Φ_i obeys a Gaussian distribution $p(\Phi_i) = \exp[-(\Phi_i - \Phi_i^0)^2/(\Delta\Phi_i)^2]$. Here, Φ_i^0 denotes the mean value of the variable Φ_i and $\Delta\Phi_i = (\langle(\Phi_i - \Phi_i^0)^2\rangle)^{1/2}$ its root-mean-square fluctuations. The transition state is assumed to require a fluctuation $\delta\Phi_j^{\mathrm{tr}} = \Phi_j^{\mathrm{tr}} - \Phi_j^0$ of those variables j which are involved in the conformational transition. Then the transition rate may be expressed as

$$k^{\mathrm{tr}} = (\tau_0)^{-1} \prod_j \exp[-(\delta\Phi_j^{\mathrm{tr}})^2/(\Delta\Phi_j)^2].$$

Here, τ_0 is the relaxation time of the fluctuations and we have assumed that the fluctuations of all variables relax with the same time τ_0. For the kinked-straight transition of the helix, only the three dihedrals (Φ_{10}, Ψ_{10}, Φ_{11}) undergo large changes at the transition, while the other variables undergo small changes within the range of their mean fluctuations (Fig. 4). For the three dihedrals (Φ_{10}, Ψ_{10}, Φ_{11}), the mean values Φ_j^0 and the mean fluctuations $\Delta\Phi_j$ in the kinked conformation were obtained as temporal averages, the $\Delta\Phi_j$ being listed in Table 1. For an estimate of the deviations $\delta\Phi_j^{\mathrm{tr}}$ of the three dihedrals at the transition point, one may inspect Fig. 1 B and choose as a rough estimate $\delta\Phi_j^{\mathrm{tr}}$ equal to half the change of Φ_j at the transition, $\delta\Phi_j^{\mathrm{tr}} = |\Phi_j^i - \Phi_j^f|/2$. Upon comparison with the mean fluctuations given in Table 1, this leads to $\delta\Phi_{10}^{\mathrm{tr}} = \Delta\Phi_{10}$, $\delta\Psi_{10}^{\mathrm{tr}} = 2\,\Delta\Psi_{10}$, and $\delta\Phi_{11}^{\mathrm{tr}} = \Delta\Phi_{11}$. Insertion into the above equation leads to $k^{\mathrm{tr}} = (\tau_0)^{-1} e^{-6} = (\tau_0)^{-1}$ 1/400. The relaxation time of the fluctuations of the dihedrals under the condition of strong coupling to a heat bath has been determined previously as $\tau_0 = 0.3$ ps (Pleiss and Jähnig 1991). Thus, one obtains for the reaction rate $k^{\mathrm{tr}} = 1/120$ ps^{-1} or for the reaction time $\tau^{\mathrm{tr}} = 120$ ps. This time is of the same order of magnitude as the time obtained from the MD simulations. Hence, the model of a random walk is at least compatible with the data from the simulations.

This model may also provide some insight into the acceleration of the transition achieved in our simulations by coupling the helix strongly to a heat bath. Under the ordinary assumption of weak coupling the fluctuations are smaller, while their relaxation time is about the same as for strong coupling (Pleiss and Jähnig 1991). As evident

Table 1. Root-mean-square fluctuations $\Delta\Phi_j$ of the dihedrals (Φ_{10}, Ψ_{10}, Φ_{11}) in the kinked conformation of the $(\mathrm{Ala})_{20}$-helix under weak and strong coupling to a heat bath at 300 K

Coupling	Weak	Strong
$\Delta\Phi_{10}$	14°	18°
$\Delta\Psi_{10}$	21°	26°
$\Delta\Phi_{11}$	22°	26°

from Table 1, under weak coupling the mean fluctuations $\Delta\Phi_j$ of the three dihedrals are smaller than for strong coupling by a factor of about 1.2. This implies, since the deviations $\delta\Phi_j^{\mathrm{tr}}$ required to reach the transition point are still the same, that the probability $p(\Phi^{\mathrm{tr}})$ is smaller by a factor of 15 and, inversely, the reaction time is longer by a factor of 15. This result again is compatible with the data from the MD simulations. So the random walk or diffusion model provides a reasonable framework for the analysis of the conformational transition observed in the MD simulations.

This finding is in general agreement with recent reports in the literature. The folding dynamics of two α-helices connected by a random-coil polypeptide chain was found to be diffusion-limited (Lee et al. 1987). The presence or absence of high energy barriers, however, was not investigated in this study. In all cases where the energy profile along a conformational transition was investigated, neither a large energy barrier seemed to be involved nor a unique reaction pathway to exist. The investigation of the folding transition of a tetrapeptide showed a large number of alternative pathways at room temperature (Czerminski and Elber 1989). Furthermore, a relatively broad distribution of relaxation times was found, which is in consonance with our result. The observation that there is no unique reaction pathway was also made in an MD study of superoxide radical diffusion in superoxide dismutase (Shen et al. 1989). During the MD simulations, the shape of the channel fluctuated considerably leading to the conclusion that the lowest energy pathway for superoxide diffusion changes permanently. A similar result was obtained recently in an MD study of CO diffusion in myoglobin (Elber and Karplus 1990). When CO escapes from the heme pocket, a variety of diffusion pathways were found. For each pathway, the barriers are of the order of thermal energy. Therefore, a single reaction coordinate is unlikely to yield a complete description. The transition is rather limited by diffusion across many small barriers than determined by a single energy barrier.

Conclusion

In MD simulations of an $(\mathrm{Ala})_{20}$-helix we observed a transition from a kinked to a straight conformation and analyzed it within the framework of different kinetic models. Our main conclusion is that the transition rate is not limited by high energy or entropy barriers, but by a random walk at about constant energy on the complex energy landscape of the peptide.

This model for the mechanism of a conformational change of a helix differs from the Kramers model for chemical reactions which has previously been introduced to describe conformational changes in proteins. The point is that the Kramers model or similar models rely on a one-dimensional reaction path. If an energy barrier occurs, the system has no chance to proceed along the path except by crossing the barrier which may take some time. In the case of a helix or a protein in general, however, the system has the possibility to circumvent the barrier due to its many internal degrees of freedom. These many degrees of freedom, on the other hand, render it difficult to reach a distinct state, the transition state. Once this point is reached, the system will approach a state of lower energy. However, to reach this point requires a long random walk since there are many possible pathways in the high-dimensional phase space and not all lead to the transition state. Thus, the rate-limiting step of a conformational transition in a peptide or protein is not to cross energy barriers, but to find a way through a high-dimensional labyrinth.

References

Ansari A, Berendzen J, Bowne SF, Frauenfelder H, Iben IET, Sauke TB, Shyamsunder E, Young RD (1985) Protein states and proteinquakes. Proc Natl Acad Sci USA 82:5000–5004

Berendsen HJC, Postma JPM, van Gunsteren WF, DiNola A, Haak JR (1984) Molecular dynamics with coupling to a heat bath. J Chem Phys 81:3684–3690

Czerminski R, Elber R (1989) Reaction path study of conformational transitions and helix formation in a tetrapeptide. Proc Natl Acad Sci USA 86:6963–6967

Dornmair K, Jähnig F (1989) Internal dynamics of lactose permease. Proc Natl Acad Sci USA 86:9827–9831

Elber R, Karplus M (1987) Multiple conformational states of proteins: a molecular dynamics analysis of myoglobin. Science 235:318–321

Elber R, Karplus M (1990) Enhanced sampling in molecular dynamics: use of the time-dependent Hartree approximation for a simulation of carbon monoxide diffusion through myoglobin. J Am Chem Soc 112:9161–9175

Frauenfelder H, Parak F, Young RD (1988) Conformational substates in proteins. Ann Rev Biophys Biophys Chem 17:451–479

Gelin BR, Karplus M (1975) Sidechain torsional potentials and motion of amino acids in proteins: Bovine pancreatic trypsin inhibitor. Proc Natl Acad Sci USA 72:2002–2006

Ghosh I, McCammon JA (1987) Sidechain rotational isomerization in proteins. Dynamic simulation with solvent surroundings. Biophys J 51:637–641

Jaenicke R (1987) Folding and association of proteins. Prog Biophys Mol Biol 49:117–237

Joseph D, Petsko GA, Karplus M (1990) Anatomy of a conformational change: hinged "Lid" motion of the triosephosphate isomerase loop. Science 249:1425–1428

Karplus M, Kushick JN (1981) Method for estimating the configurational entropy of macromolecules. Macromolecules 14:325–332

Karplus M, Weaver D (1976) Protein-folding dynamics. Nature 260:404–406

Kramers HA (1940) Brownian motion in a field of force and the diffusion model of chemical reactions. Physica 7:284–304

Lee S, Karplus M (1988) Dynamics of reactions involving diffusive multidimensional barrier crossing. J Phys Chem 92:1075–1086

Lee S, Karplus M, Bashford D, Weaver D (1987) Brownian dynamics simulation of protein folding: a study of the diffusion-collision model. Biopolymers 26: 481–506

Northrup SH, Hynes JT (1980) The stable states picture of chemical reaction. I. Formulation of rate constants and initial condition effects. J Chem Phys 73:2700–2714

Northrup SH, Pear MR, Lee CY, McCammon JA, Karplus M (1982) Dynamical theory of activated processes in globular proteins. Proc Natl Acad Sci USA 79:4035–4039

Piela L, Nemethy G, Scheraga WA (1987) Proline-induced constraints in α-helices. Biopolymers 26:1587–1600

Pleiss J, Jähnig F (1991) Collective vibrations of an α-helix. A molecular dynamics study. Biophys J 59:795–804

Roder H, Elöve GA, Englander SW (1988) Structural characterization of folding intermediates in cytochrome C by H-exchange labelling and proton NMR. Nature 335:700–704

Ryckaert JP, Ciccotti G, Berendsen HJC (1977) Numerical integration of the cartesian equations of motion of a system with constraints: molecular dynamics of *n*-alkanes. J Comp Phys 23: 327–341

Schulten K, Schulten Z, Szabo A (1981) Dynamics of reactions involving diffusive barrier crossing. J Chem Phys 74:4426–4432

Shen J, Subramaniam S, Wong CF, McCammon JA (1989) Superoxide dismutase: Fluctuations in the structure and solvation of the active site channel studied by molecular dynamics simulation. Biopolymers 28:2085–2096

Udgaonkar JB, Baldwin RL (1988) NMR evidence for an early framework intermediate on the folding pathway of ribonuclease A. Nature 335:694–699

Van Gunsteren WF, Karplus M (1982) Effect of constraints on the dynamics of macromolecules. Macromolecules 15:1528–1544